

Central European Journal of Physics

Organization of matter into one-dimensional units on designed media

Research Article

Karen B. Paul*

Hephaistos Nanotechnology Research Center, University of Cyprus, 75 Kallipoleos Ave, PO Box 20537, 1678 Nicosia, Cyprus

Received 14 September 2010; accepted 21 December 2010

Abstract:

The organization of magnetic materials into one-dimensional micro- and nanowires on designed media is discussed, exemplified by two experiments on the microscale and nanoscale, with regard to particles as basic building blocks for the growth and development of matter.

In the first organizational experiments, cobalt (Co) micro-particles are assembled on patterned media with perpendicular magnetization by acoustic vibrations onto designed shapes reflecting macroscopically the parent material. In the second experiments, semiconductor Germanium-Dysprosium (Ge₉₈Dy₂) matter is assembled on gold (Au) catalytic nuclei in a tube reactor by physical vapor transport as clusters of nanowires.

The underlying mechanisms of organization are described, and similarities and distinctive features in the processes are discussed. The role of the energy-input in the form of mechanical vibrations and heat is outlined with its similar impact on the assembly and growth of matter on surfaces. The description of these experiments in view of organization allows more control over the processes of planned arrangement on designed media. Routes for further progress in this direction are briefly outlined.

PACS (2008): 81.07.-b, 62.23.c, 75.50.-y, 75.50.Pp

Keywords: structured materials • magnetic assemblies • nanowires • clusters • dilute magnetic semiconductor

© Versita Sp. z o.o.

1. Introduction

The arrangement of micro and nano-objects on patterned media emerges within the contemporary organizational methods and techniques [1–3] applied in nanotechnology. Its purpose is to create independent entities with a unique blend of properties, some inherent from the parent material, some intrinsic, originating from the smallest unit, and

blended into a new complex variety. Organization on patterned surfaces encompasses broadly the participation of the smaller organized units into a larger formation with pre-designed, or at least expected physical properties.

The process may produce the result as an entity, containing both the substrate and the organized particles. Alternatively, the organized material may be separated as an independent unit. The newly created morphology on the parent material is metastable. Consequently, when the powder-material is separated from the substrate, the particulate structure may transform into a different morphological unit, possibly preserving some macro-properties,

^{*}E-mail: dr_kpaul@hotmail.com

such as the intrinsic saturation magnetization, and the extrinsic remanence and coercitivity.

Organization of particles on patterned media may be utilized to enhance and modify the inherent properties of the substrate, e.g. in the case of perpendicularly magnetized Co/Pt [4] or Fe/Pt [5] patterned surfaces, organized Fe_3O_4 particles will add to the inherent magnetic properties of the substrate. In another instance, entrenched and organized nanowires in antidots [6] will lead to in-situ fabrication of nano-devices with targeted properties [7].

In view of the distinct processes of assembly and growth, we will discuss in this work two types of organizational experiments. In the first, magnetic micro-particles, as basic model-units of growth, are organized into magnetic whiskers and shaped as macro-objects on vibrating patterned media with inherent perpendicular magnetization. In the second experiments, the matter as evaporated nano-droplets is organized as nanowires within microclusters, on substrates with gold (Au) catalysts in a tube reactor. The organizational process is conductive through chemical vapor deposition (CVD), in particular, thermal vapor transport [8]. (The basic building block for the growth is a nano-particle, the resulting nano-unit is a nanowire, incorporated in larger designed micro-clusters on the surface.)

Many factors influence the organizational process, but among them there are two that are most essential and related to the two interacting parties: the surface on which the matter is organized, and the matter which is organized. The cleanness of the substrate, its various treatments, environmental conditions such as moisture or pressure affect the motion of the particles on the surfaces.

Also the nature and inherent properties of the matter to be organized, such as size, shape, dielectric and magnetic properties, have an impact on the character of the motion on the surface, especially on the microscale and below [9]. In particular, the nature of the friction on the surfaces is dependent on the attributes of the particles, clusters or agglomerates. Therefore, it will affect the adhesion, paring and clustering of the material [9]. Thus, the processes on the surfaces shape indirectly the morphology and the physical properties of the produced structure.

In the second example for organization in a tube reactor, the thermodynamics is described with the following parameters: volume of the tube (V), pressure (P) in the reactor, temperature of the evaporated material (T), temperature of the substrate for the deposited material (T_1) , and gas-flow rate (v) [8]. While T, V and P are interdependent, v and T_1 are independent, and they may be chosen within reasonable limits defined by the objectives, such as physical type and size of the deposited matter on the designed substrates: particles, nanowires, clusters,

and thin films.

The goal of this work is to analyze the underlying mechanisms of the organization of matter on surfaces based on these two experiments, and seek routes for actively influencing the processes of assembly, self-assembly, growth and quality of the entities on the substrates.

2. Experimental

In the first experiments, cobalt (Co) powder with average particle diameter 1.6 μ m was spread on a surface and organized by externally imposed mechanical vibrations on the designed patterns with inherent perpendicular magnetization.

Amorphous FeCoS ribbon with a perpendicular magnetic component was cut and shaped under a microscope into various designs, and Co particles were spread on transparent non-magnetic paper placed on the model.

The magnetic patterns were subjected to vertical vibrations with amplitudes (A) $\leq 2~\mu m$ and frequencies sweeping in the acoustic range between 10 Hz and 10 kHz. The vibrations were generated by a low-voltage actuator, type PA 4/12 (Piezosystem Jena Inc.¹), fed by a power supply ENV800¹. The sample-holder, attached accordingly to the actuator, conveyed the vertical vibrations to the particles. (For details see Fig. 1 of Ref. [9].)

The final materials produced were particulate assemblies of various shapes and thicknesses $\approx 1~\text{mm}.$

The morphology of the fabricated structures was studied by scanning electron microscopy (SEM) utilizing a TESCAN VEGA/LM microscope. Macro-magnetic measurements such as room-temperature hysteresis were conducted by a vibrating sample magnetometer (VSM Lakeshore) to compare the physical properties of these materials with the properties of the pads and to relate to the overall organizational processes.

In the second experiments the matter in the form of $Ge_{98}Dy_2$ alloy-nanowires is organized by Au growth catalysts on a substrate with the assistance of externally imposed Ar gas-flow and the temperature of the Au nuclei. The source of the nanowires is powder-material, accommodated in a sealed tube reactor with length 1 m and

modated in a sealed tube reactor with length 1 m and diameter 2.5 cm (1 inch), in Ar atmosphere. Details for some fabricated and treated GeDy alloys are described in Ref. [10].

The Au nuclei were produced on commercial $Si(100)/SiO_2(300 \text{ nm})$ wafers by electron beam evapora-

¹ Peizosystem Jena Equipment for Nanopositioning, http://www.piezojena.com

tion of 2 nm Au, using an evaporation rate of 0.2 Å/s. The substrates were subsequently heat treated for 30 min in a vacuum at $\approx 450^{\circ}\text{C}$ to form Au islands. Their average size ($\approx 60~\mu\text{m}$) is determined by the conditions of their fabrication — evaporation rate, thickness of the Au film, length and temperature of the heat treatment.

The parameters of the deposition process of the nanowires were adjusted according to the dimensions of the tube reactor to actualize a non-equilibrium, low-pressure, static thermodynamic process. Specifically, the Ar gas pressure was 2.93×10^4 Pa (300 mbar), the Ar gas flow-rate was 200 standard cubic centimeters per minute (sccm), the temperature of the Ge98Dy2 powder-source was 900°C, the temperatures of the substrates with Au nuclei were 500°C and 550°C, and the deposition time was 10 minutes.

The structural quality (XRD) of the nanomaterials was studied by a Shimadzu 6000 diffractometer, their morphology by a TESCAN VEGA/LM microscope, the qualitative and quantitative composition by EDX (Energy-dispersive X-ray spectroscopy) with a detector attached to the SEM, and phase purity and a basic magnetic property – thermoremanent magnetization (TRM), by QD MPMS-4. There characteristics were recorded to relate the physical attributes of the materials with the processes of growth and development in the CVD chamber.

3. Results and discussion

3.1. Organization of Co particles into artificial structures by acoustic vibrations

Two of the forces acting in the first organizational experiments can be defined broadly as interparticle (intercluster), and static-magnetic force of attraction between the parent material and the particles. In addition to these forces, a mechanical vibration is initiated from the piezo system, and imposed on the particulate matter.

The Co particles used in this work are polydomain and not-separated, therefore, they are able to cluster. Moreover, the interparticle interactions in a cluster are dipolar, i.e. attractive, which may lead to its further agglomeration. The intercluster interactions reflect on a larger scale the interparticle interactions. When the exchange coupling anisotropy of two clusters is greater than the demagnetizing (dipolar) anisotropy, the clusters are able to pair on a larger scale [11]. Thus, they can couple on a surface to produce agglomerates of various sizes and shapes.

The patterned substrate acts on the clusters with a vertical, static, magnetic attractive force, which keeps them spread all over the surface without following any particular design.

The clusters are subjected to a mechanical force (F) by the vibrating surface:

$$F = mAf^2 \cos(2\pi f t). \tag{1}$$

In Eq. (1) m is the mass of a particle or a cluster, t is the time-period of the vibration, and A and f are the amplitude and the frequency of the vibration. When the energy associated with the force F becomes commensurate with the inter-cluster exchange energy, the vibrations may interfere in the clustering process. They may prevent further increase in size by breaking the clusters down into smaller clusters and tossing away the large agglomerations. This becomes possible above certain values of the amplitude A and above a critical mass of the clusters according to Eq. (1) and results in Ref. [9].

The particles are placed in the vertical magnetic field of the patterned medium, and this facilitates the arrangement of the clusters on the designed pattern after a sufficient total time of the imposed vibrations. The total time needs to be adequate for optimization of the parameters of the replica: the total mass, geometrical dimensions and density of the particles.

In Fig. 1 are displayed some structures created using this method of organization. In Fig. 1a an image is displayed of an assembly of Co particles situated on a modeled horseshoe, and in Fig. 1b the picture of another assembly is presented. Both images are taken with a camera attached to an Olympus BX51M microscope, and they magnify the original 50 times ($50\times$). Morphological detail in the structures is not clearly seen in Figs. 1a and 1b, which necessitated the use of more advanced microscopy. Fig. 1c presents an SEM image of a basic $3 \text{ mm} \times 1 \text{ mm}$ Co-particle assembly. Details are clearly observed – the structure of particles consists of magnetic whiskers, some pointing outside the sample plane, and well seen along the pole-line of the parent material. Presented in Fig. 1d is another artificial structure built on four closely situated small magnetic pads; the neighboring whiskers in the assemblies are connected and form stripes of particles.

An important result of these organizational experiments is the reproducibility of the induced geometrical parameters — length, width, height, within a total error $\leqslant 5\%$. The morphology of the replicas is also satisfactorily reproduced when the structure is on the magnetic pad. These results can be explained with the interplay of the acting forces, which create a metastable structured material. Its existence depends significantly on the substrate, and it is achieved with a sufficient quantity of powder on the vibrating system and time of vibrations ≈ 10 min to reach the mass-saturation value. The excessive powder is tossed away, and a self-sustained replica of the original is produced.

The materials were packed carefully under the microscope for various macro-property measurements which results in assumptions about their morphology and local micro properties inside the package.

The assemblies are with induced shape anisotropy which influences their performance.

Magnetic characteristics of the fabricated structured materials with widths 1 mm and lengths varying from 1 mm to 6 mm, measured and compared with the inherent properties of the pads, are displayed in Fig. 2.

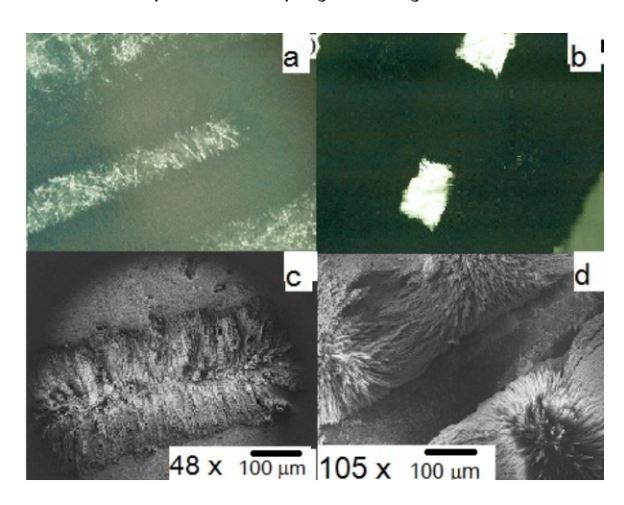


Figure 1. (a) and (b): Photo-images of various assemblies of Co particles (50×) taken with a digital camera attached to an Olympus BX51M microscope; (c) an SEM image of a 3 mm × 1 mm structure of Co-particles (d) an SEM picture of two particle-stripes, situated on four small, closely positioned magnetized pads.

Exemplary magnetic hysteresis measurements at $300~\mathrm{K}$ for the sample with dimensions $3~\mathrm{mm} \times 1~\mathrm{mm}$, assembled on a rectangular substrate, are shown in Fig. 2a for the parallel (par) and perpendicular (per) orientations of the sample-plane to the applied magnetic field.

The coercitivity, remanence and squareness of the hysteresis loops in Fig. 2a are lower compared to those of the parent material, presented in Fig. 2b. However, for both materials, the calculated ratios

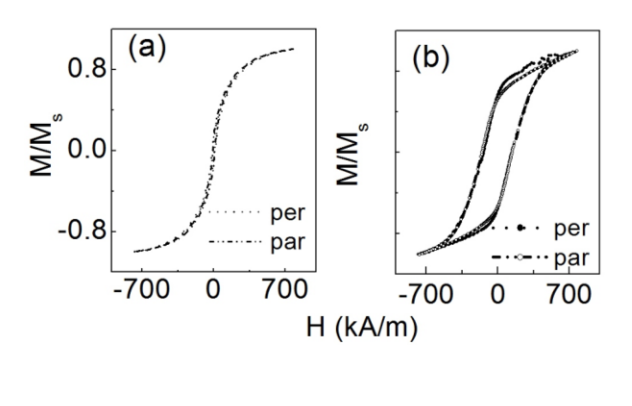
$$\frac{H_{\rm c}^{\rm per}}{H_{\rm c}^{\rm par}}$$

are approximately equal, and the switching properties are nearly isotropic in-plane.

In Fig. 2c the low-field part of a hysteresis loop for the 3 mm \times 1 mm assembly is displayed; a distinctive, double-jump behavior is observed for all samples longer than 2 mm when oriented parallel to the magnetic field.

The incoherent switching in external parallel magnetic field [12] is possibly due not only to the geometrical aspects of the patterned medium, but also to its singular properties [13]. There is a magnetic pole area in the parent material which results in non-homogeneous distribution of the particles on the sample-plane as seen in Figs. 1c and 1d. Although a general principle of minimizing the surface area of the poles is valid, the non-homogeneity may affect the macro-properties, which are better detectable with longer (larger) samples.

In Fig. 2d the dependencies of the coercive fields $H_{\rm c}$ of the replicas on the changing geometrical dimension (length L) are presented. For all structures the measurements resulted in higher coercitivities out-of-plane and magnetic remanence that was twice lower, as compared to the corresponding in-plane parameters, similar to the performance of the parent material.



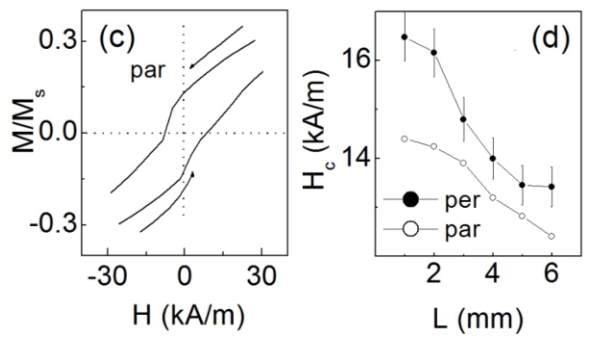


Figure 2. (a) M(H) plots at 300 K for the sample with dimensions 3 mm \times 1 mm, measured in perpendicular (per) and parallel (par) orientation to the magnetic field. (b) The related characteristics of the pad. (c) The details of a hysteresis plot in the low-field range for a 3 mm \times 1 mm sample. (d) $H_c(L)$ for the replicas. The dark circles are presented with 3% error bars, and represent $H_c(L)$ for perpendicular orientation of the sample plane. The open circles represent $H_c(L)$ for the parallel plane. The lines serve to guide the even

Thus, the fabricated structures are low-remanent, and exhibit perpendicular magnetic anisotropy and near — in-plane isotropy, similar to the parent materials.

With this type and size of particles, range of the applied frequencies and amplitude of the piezo-element vibrations, the obtained macro-magnetic characteristics were remarkably reproducible within the sensitivity of the instrument (VSM $\sim 10^{-6}$ emu). This is partially due to the relatively good reproducibility of the geometrical dimensions of the structure. With Co particles of a smaller diameter, it is possible to achieve alternative, improved and planned macro-characteristics at mass saturation values of the assemblies.

3.2. Organization of matter in a tube reactor

The objective of this section is to describe fabrication of nanowires by physical vapor transport within the approach of the organization of matter on media. Similarities and distinctive features from the processes in part 3.1 will be outlined and discussed.

The processes in a chamber can generally be classified as internal, and externally controlled. The first generate the matter, and the latter organize it on the patterned medium. (This classification is broad and contingent on the details of fabrication of the materials.)

The internal parameters P, V and T_{av} jointly contribute in producing matter with a total mass proportional to

$$\frac{PV}{T_{ave}}$$

in the form designed for the process in the chamber – droplets, clusters, nanowires or thin layers, in thermodynamic non-equilibrium steady-state conditions. (T_{av} is the average temperature in proximity of the temperature-point set to T, according to the design of the tube furnace; the length of the averaged temperature region is ≈ 10 cm.) Conditions for various processes can be created by the interplay of the three factors, e.g. low-pressure or high pressure experiments with evaporation or sublimation of the principal matter, correspondingly [8].

The catalysts for the nanowire growth, the Ar (or other) gas-flow, and the temperature of the substrate (T_1) are the externally adjustable organizing factors.

Fabrication of the Au nuclei-seeds seems to be one of the most elaborated, sometimes underestimated steps in the process of Ge-based nanowire growth [2]. On the microscale, it influences the growth of the clusters with nanowires, on the nanoscale – the quality and size of a nanowire [2].

Preparation of the Au nuclei encompasses important preliminary treatments of the Si substrate following the standard RCA (reactor control assistance) pre-cleaning². Various pretreatments of the Si surfaces are described in the literature; some of them are the oxygen (O) and hydrogen (H) – terminations discussed in Ref. [14]. It is established that the growth mode of gold is significantly affected by them since the surface morphologies are changed. For example, the Au ad-atoms nucleate and agglomerate to form stable islands on oxygen-terminated SiO_2 substrates, while on hydrogen-terminated Si surfaces the Au atoms form a wetting layer [14].

In this work commercial $Si/SiO_2(300\ nm)$ wafers are used, cleaned in acetone and treated in 2% HF (hydrofluoric acid) for 1 min.

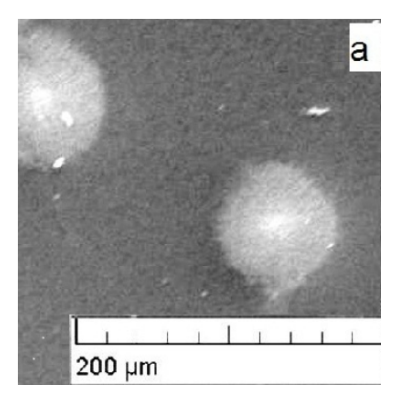
The growth techniques employed for the Au seeds vary in the literature [2, 14–17]. For example, in Ref. [15] the sol-gel method is used with HAuCl₄ as a precursor, in Ref. [16] thermal evaporation of Au is applied, in Ref. [17] – sputtering, and in Refs. [2, 14] – electron beam evaporation. The analyses for homogeneity of size and shape of the fabricated Au islands by various techniques conclude in favor of electron beam evaporation as the most adequate [2, 14–17], and this is therefore also applied in this work.

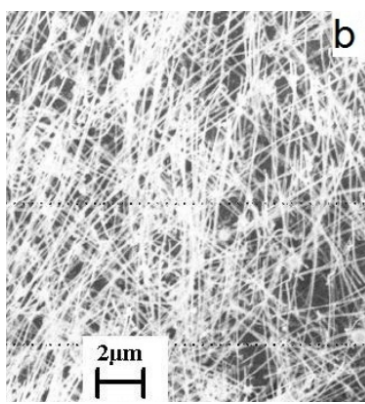
The thicknesses of the e-beam evaporated gold are usually between 0.5 and 2 nm [2, 14]. Post annealing of Au/SiO $_2$ is utilized for size homogenization [16]. Post-termination of Au, grown on H-terminated Si is applied for 2 min in 1.5% HF to remove the SiO $_2$ overlayer which appears as a result of Si diffusion [14]. The temperature and time-length of the post annealing should be carefully monitored, especially in the case of patterned small areas with Au deposits to prevent additional clustering, characteristic for Au on SiO $_2$ at elevated temperatures [18].

The Au nuclei control *the position* of nanowire growth³. Their size determines the size of the clusters with nanowires [2]. The surface roughness of the fabricated Au seeds influences the kinetics of growth of a single nanowire [14].

The *density* of the nanowires is controlled in three ways: by H-pretreatment of the Si surface [14], by decreasing the size of the Au seed down to 10 - 12 nm with one nanowire on it [2], and by external adjustment of the partial

 ² C.B. Li, K. Usami, H. Mizuta, K. Uchida, S. Oda, Repository of University of Southampton [School of Electronic and Computer Science] UK (2008) http://eprints.ecs.soton.ac.uk/16745/1/cpaper_163.pdf
³ C.B. Li, K. Usami, H. Mizuta, K. Uchida, S. Oda, Repository of University of Southampton [School of Electronic and Computer Science] UK (2008) http://eprints.ecs.soton.ac.uk/16269/1/cpaper_147.pdf





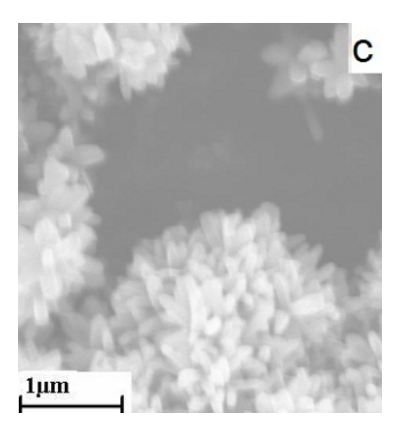


Figure 3. (a) An SEM image of clusters of nanowires on Au seeds. (b) A detailed SEM image inside a cluster. The nanowires are of diameter ≈ 30 nm, and they are produced on substrates placed at ≈ 500°C. (c) Clusters of nanowires produced at 550°C.

pressure of the precursor, (10% GeH_4^4), while keeping the total pressure with the H_2 gas⁴ constant.

The density of the nanowires in our experiments is monitored by adjusting the temperature T, at which the source powder is situated. According to the binary phase diagram of GeDy [19], at low Dy concentrations, there is a narrow operative temperature range of $\Delta T \approx 80$ degrees

starting from 860°C up, throughout which $\text{Ge}_{98}\text{Dy}_2$ gradually undergoes solid-liquid-gas (SLG) phase transitions. (The starting point of this temperature range is contingent upon the pressure in the chamber.) At the high temperature points of this interval the evaporation is more vigorous and produces nanowires of higher density⁴. Both controls of the density of the nanowires operate similarly by changing the partial pressure of the actual substance-carriers and preserving constant the total pressure of the gas in the chamber.

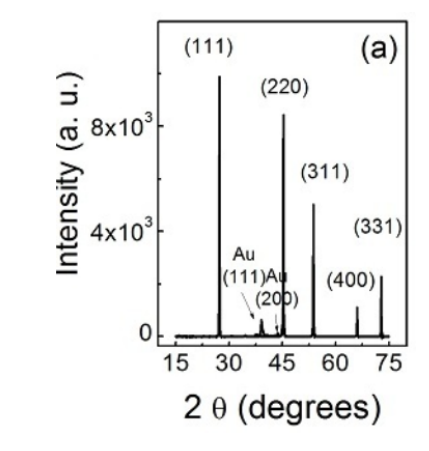
The axial growth speed of a nanowire is controlled by the temperature T_1 of the nucleation seeds, which is usually determined by their position in the tube-reactor. The produced nanowires have a larger diameter but different morphology⁴, if the substrate is placed at a temperature 50 degrees higher (see e.g. Fig. 6⁴). Examples of influenced axial growth are the specific crystalline growth characteristic for a temperature T_1 or the non-specific decomposition of GeH_4 at $350^{\circ}C^4$. The possibility of the rearrangement of the Au nuclei on the surfaces at elevated temperatures should also not be underestimated [18], this may modify the originally created structure, and consequently the parameters of the nanowires. A precise monitoring of the temperature T_1 will make the production of the nanowires more size-sensitive.

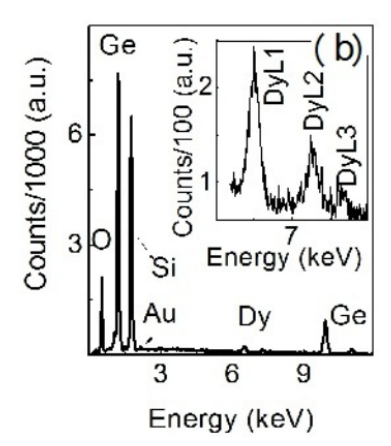
The *time* of deposition is also an essential factor, primarily for the length of the nanowires⁴. C.B. Li, et al. report on a presence of thick-and-short wires on the substrate alongside with thin-and-long, corresponding to a one hour time of deposition. The long time of deposition is possibly one reason for the growth of thick-and-short nanowires beside the thin. The effective temperature \mathcal{T}_1 presumably increases due to the bombardment with hot matter from the source, thus causing variations in size of both seeds and wires.

The time used to prepare the nanowires in the presented results is 10 min.

Powdered material from a $Ge_{98}Dy_2$ ingot, made by arc melting and appropriate heat treatments [10], is placed in the tube reactor at the position corresponding to $900^{\circ}C$. Special antioxidation measures were taken during the fabrication of the pellet, preparation of the powder for the nanowires, and its transportation to the tube reactor. The substrates with Au nuclei were placed at the positions corresponding to $500^{\circ}C$ and $550^{\circ}C$ in subsequent experiments.

⁴ C.B. Li, K. Usami, H. Mizuta, K. Uchida, S. Oda, Repository of University of Southampton [School of Electronic and Computer Science] UK (2008) http://eprints.ecs.soton.ac.uk/16745/1/cpaper_163.pdf





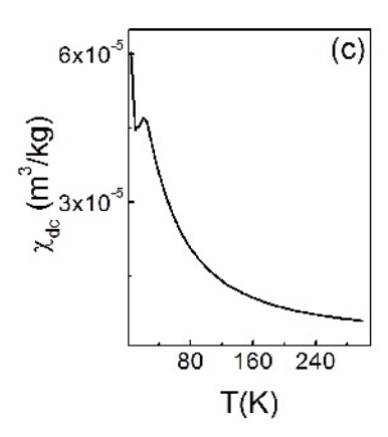


Figure 4. (a) An XRD pattern of nanowire material; (b) An EDX spectrum acquired with an SEM, supplied with a detector. In the inset is displayed the magnified part of the spectrum between 6 keV and 8 keV with DyL1, DyL2 and DyL3-peaks; (c) TRM (T).

The nanowires were prepared in a flowing Ar atmosphere in the conditions described in the Experimental Section. The average evaporated mass is ≤ 0.03 mg/min.

In Fig. 3a an image of clusters of nanowires produced at 500°C is displayed. The average estimated diameter of a cluster is 70 μm in accordance with the diameter of a catalyst seed ($\approx 60~\mu m$). In Fig. 3b are presented details within a cluster, produced at 500°C: size homogeneity of the nanowires, average diameter $\approx 30~nm$, length $\approx 4~\mu m$, and calculated axial growth rate $\approx 400~nm/min$.

An image of the clusters of nanowires fabricated at 550°C is displayed in Fig. 3c. The Au seeds are more inhomogeneous in size, the nanowires are shorter (300 nm) and thicker (100 nm), and the calculated axial growth rate is pprox 30 nm/min. The inhomogeneity of the clusters, the modified dimensions of the nanowires, and their reduced axial growth are possibly consequences of the increased temperature of growth T_1 . It will be insightful to investigate precisely the range around a temperature T_1 , for which the thermodynamic processes include the conservation of the mass (or volume) of a nanowire. The non-dissipative processes cover a variety of nanowire sizes within the multiplicity of semi static thermodynamic conditions. Such investigation will shed light on the axial growth, optimal conditions for it, and possible crystalline phases and morphology of growth on the nanoscale.

The nanowires from Fig. 3 were characterized, and some results are displayed in Fig. 4. In Fig. 4a an XRD pattern of the nanowires fabricated at 550° C is presented, in Fig. 4b is their EDX spectrum, and in Fig. 4c – is the temperature dependence of the TRM(T).

The XRD results revealed the unaffected crystalline lattice parameter (a) of the new alloy material GeDy₂, $a\approx 0.5661$ nm, similar to the results in Ref. [17] for the GeMn₅ nanowires. This seems attainable at low concentrations of the dopant, even when its atomic radius ($R_{\rm Dy}$) is substantially larger than that of Ge, in the case:

$$\frac{R_{\rm Dy}}{R_{\rm Ge}} \approx 1.45.$$

The quantitative analyses from the EDX spectra recorded from different points of the samples revealed the presence of Dy in the nanowires. Due to the error of the method, $\approx 5\%$, it is possible that the amount of Dy was different from the designed 2 at %. Any changes in the concentrations of the constituents (Ge and Dy) can be ascribed to the aggressive steps in the fabrication procedure: the arc-melting and the conditions of the heat treatment of the bulk material [10].

The thermoremanent measurements are often used as a sensitive method above the capabilities of XRD to verify phase composition or observe possible phase transitions. Fig. 4c presents the temperature dependence of the thermoremanent dc mass magnetic susceptibility, $\chi_{\rm dc}(T)$. Based on estimations of the Curie-Weiss (CW) constant

and CW temperature T_c , a conclusion is drawn that the materials are paramagnetic above 20 K, and disordered, spin-glass-like, superparamagnetic below 20 K.

It seems viable according to theoretical work [20–22] that at an appropriate concentration of Dy ($x\approx 10$ at %) [20], the $Ge_{100-x}Dy_x$ material as nanowires will exhibit a well-developed, soft-ferromagnetic state with considerable coercitivity and remnant magnetization at room temperature.

The scope of this work, however, is on the organization of matter and the common mechanisms in seemingly different methods and scales. We introduced a new Ge₉₈Dy₂ semiconductor nanowire material, and discussed its fabrication and influencing instruments on the nanoscale, considering possibilities to use similar highly doped Ge-based nanowires as room temperature magnetic semiconductors and magnetic nanodevices. The last aspect will complement partially achieved goals to orient a nanowire in a desired direction [7, 14]. A single magnetic nanowire will be easily directed in a relatively small switchable magnetic field in an appropriate environment; analogously, a dielectric nanowire – in an electric field.

4. Discussion and conclusions

It is much discussed in technology, that growth mechanisms are essential for the quality and functionality of materials. Organization and growth are two basic, but different, intermixed processes.

In a qualitative description of the *controlling* tools in the presented experiments, the Ar gas-flow, the temperature of the nuclei \mathcal{T}_1 , and the Au catalysts in 3.2 are associated with the particle-flow, frequency of the vibrating piezo system, and the magnetic patterned medium in 3.1, correspondingly.

The Ar-gas flow delivers the matter to the nuclei in the nano-experiments, and a similar activity is executed by the person performing the micro-experiments via dispersing the particles on the substrate, thus controlling the particle-flow. The temperature of the substrate \mathcal{T}_1 in the reactor chamber is similar to the function of the mechanical vibrations of the piezo system. At a critical frequency, the vibrating system will toss away the large clusters and keep on the surface of the patterned magnetic material only those compatible. Similarly, if the temperature \mathcal{T}_1 is higher than a critical value, the landed matter on the substrate with the Au seeds will re-disperse, and a growth process will not be initiated.

The catalytic Au islands in the organization of $Ge_{98}Dy_2$ material locate the clusters with the nanowires, similarly to the magnetic pads which attract the Co particles in

organizing them into magnetic whiskers. Both are starting points for the growth and development of the materials on them and their quality is essential throughout the process of organization and for the future performance of the structured material. However, their influence ends in the 2-D growth and arrangement, mainly. The third dimension is governed by the processes in the chamber (correspondingly the environment in the acoustic assembly experiments), and depends on the nature, state and local particle-interactions of the deposited material. The artificial Co whiskers created in ambient pressure and temperature, are in a fragile metastable state a function of the interplay of the local acting forces and the statistical-mechanical distribution of the matter on the patterned medium. The Ge₉₈Dy₂ nanowires deposited in chamber pressure at temperature T_1 are comparatively independent of the substrate. However, the growth process is catalyst-dependent as compared to the catalyst-free nanowire production by the Selective-Area Metal Organic Vapor Phase Epitaxy (SA-MOVPE) [23]. In SA-MOVPE the dependence on the attributes of the substrate is more pronounced, but compensated for by better orientation and size control of the nanowire [23].

In the acoustic experiments the particulate matter is assembled to form magnetic whiskers which interact on the microscale. The matter is organized in the existent form, distinctively from the experiments in the reactor.

In the vapor transport – experiments, the particulate matter undergoes SLV phase transitions, and it is assembled as nanowires in the conditions employed in the chamber.

There is no real growth process in the Co-whiskers; the process is an induced assembly, while with the $Ge_{98}Dy_2$ nanowires the processes are assembly *and* growth.

Thus, the controls in the acoustical assembly of matter are operated through regulation of the particle-flow to the substrate, fine-tuning of the frequency and amplitude of the piezo-vibration, precision of the pattern design and improved qualitative characteristics of the base magnetic medium. Accordingly on the nanoscale, the controls of the processes in the reactor chamber are utilized by adjusting the Ar-gas flow, the temperature of the substrate \mathcal{T}_1 , and the design and quality of the Au seeds, down to the nanoscale.

A goal in nanotechnology is production of autonomous nano-materials and devices with minimized influence of the base materials, such as substrates and catalysts, to ensure optimized controlled functioning of the output. A way to achieve this goal is by approaching the nanoworld from macro (thin layers) to micro on designed media, and to nano. Along this trend of optimization and miniaturization is the organization of matter on media, with clear understanding of the underlying mechanisms of growth.

In conclusion, the description of the organizational experiments allows more control over the processes in planned arrangement on designed media. Two seemingly very different examples of organization were used to approach the problem from the microscale down to the nanoscale. The underlying mechanisms are associated, and it was shown that they have similar impact on the organization of matter. The specifics of the fabrication of magnetic structured assemblies in ambient surroundings are exemplified for organization on the microscale. Production of the new non-magnetic semiconducting $Ge_{98}Dy_2$ nanowires by physical vapor transport in a tube reactor is illustrated for the processes on the nanoscale. Reduced possibility for axial growth is demonstrated, and conditions for optimal growth at a seed are briefly discussed.

Organization is approached also, in this work and analyses from the scope and level of induced assembly (without real growth) to organization with growth and development of a new material. As a result of the analyses, the Ar gas flow, similarly to the particle flow can be regarded as a step-one organization-control parameter, while the temperature of the catalysts T_1 , similarly to the frequency of the vibrations (f) can be classified as step-two in the hierarchy of organization. Ultimately, the magnetic pads and the Au catalysts are entirely growth control factors - step 3 in the organizational hierarchy. None of these steps, taken separately, or in pairs, can create a material independently. The parameters f and T_1 have a supportive, intermediate and lifting role in the hierarchy between steps 1 and 3. Their input as mechanical or heat energy, in these particular examples, directs and conducts a higher level of organization than a simple assembly. Moreover, this energy-input partially determines the type and quality of the grown material, and therefore shifts the organizational hierarchy along the spiral of the development of matter.

Acknowledgements

The author acknowledges funding support from the Cyprus Research Promotion Foundation – NanoCyprus.

References

- [1] J.C. Lodder, J. Magn. Magn. Mater. 272-276, 1692 (2004)
- [2] C. Li et al., Appl. Phys. Express 2, 015004 (2009)
- [3] Z.W. Pan, S. Dai, D.H. Lowndes, Solid State Commun. 134, 251 (2005)
- [4] K.K.M. Pandey, J.S. Chen, J.F. Hu, G.M. Chow, J. Phys. D Appl. Phys. 42, 015009 (2009)
- [5] M. Watanabe, M. Homma, Jpn. J. Appl. Phys. 35, L1264 (1996)
- [6] C.C. Wang, A.O. Adeyeye, C.C. Lin, J. Magn. Magn. Mater. 272-276, E1299 (2004)
- [7] J. Li, C. Lu, B. Maynor, S. Huang, J. Liu, Chem. Mater. 16, 1633 (2004)
- [8] J.E. Crowell, J. Vac. Sci. Technol. A 21, S88 (2003)
- [9] K.B. Paul, Rev. Sci. Instrum. 80, 85110 (2009)
- [10] K.B. Paul, G.I. Athanasopoulos, C.C. Doumanidis, C. Rebholz, Adv. Condens. Matter Phys. 2010, 107192 (2010)
- [11] G. Herzer, In: K.H.J. Buschow (Ed.), Handbook of Magnetic Materials, vol 10 (North Holland, Elsevier Science, Amsterdam, 1997) 415
- [12] L. Torres, E. Martinez, L. Lopez-Diaz, J. Iniguez, J. Appl. Phys. 89, 7585 (2001)
- [13] R.P. Cowburn, D.K. Koltsov, A.O. Adeyeye, M.E. Welland, Europhys. Lett. 48, 221 (1999)
- [14] C.B. Li, K. Usami, T. Muraki, H. Mizuta, S. Oda, Appl. Phys. Lett. 93, 041917 (2008)
- [15] A.R. Phani, V. Grossi, M. Passacantando, L. Ottaviano, S. Santucci, In: NSTI (Ed.), Technical Proceedings of 2006 NSTI Nanotechnology Conference and Trade Show, 7-11 May 2006, Boston, USA (NanoScience & Technology Inst., Cambridge, MA, USA, 2006) 141
- [16] G. Gu et al., J. Appl. Phys. 90, 5747 (2001)
- [17] Y.J. Cho et al., Chem. Mater. 20, 4694 (2008)
- [18] J.A. Venables, J. Vac. Sci. Technol. B 4, 870 (1986)
- [19] T.B. Massalski, H. Okamoto, In: T.B. Massalski (Ed.), Binary Alloy Phase Diagrams, vol 2 (ASM International, New York, 1986) 132
- [20] E.Z. Meilikhov, Phys. Rev. B 75, 045204 (2007)
- [21] D.J. Priour Jr., S. Das Sarma, Phys. Rev. Lett. 97, 127201 (2006)
- [22] T. Dietl, J. Phys.-Condens. Mat. 19, 165204 (2007)
- [23] H. Goto et al., Appl. Phys. Express 2, 035004 (2009)